Inorg. Chem. **2006**, *45*, 7069–7076

Chiral Magnetic Metal-Organic Frameworks of Dimetal Subunits: Magnetism Tuning by Mixed-Metal Compositions of the Solid Solutions

Ming-Hua Zeng,[†,§] Bo Wang,[†] Xin-Yi Wang,[‡] Wei-Xiong Zhang,[†] Xiao-Ming Chen,*[,†] and Song Gao*[,‡]

MOE Key Laboratory of Bioinorganic and Synthetic Chemistry, State Key Laboratory of Optoelectronic Materials and Technologies, School of Chemistry and Chemical Engineering, Sun Yat-Sen University, Guangzhou 510275, P. R. China, Beijing National Laboratory for Molecular Sciences, State Key Laboratory of Rare-Earth Materials Chemistry and Applications, College of Chemistry and Molecular Engineering, Peking University, Beijing 100871, P. R. China, and Research Institute of Bioinorganic Chemistry, Department of Chemistry and Chemical Engineering, GuangXi Normal University, Guilin 541004, P. R. China

Received March 27, 2006

The isostructural, chiral molecular magnetic materials with the formula $[M_xM'_{2-x}(ca)_2(1,4\text{-dimb})]_n$ [H_2ca = *D*-(+)-camphoric acid, 1,4-dimb = 1,4-di-(1-imidazolyl-methyl)-benzene, M = Ni^{II}, M′ = Co^{II}, $0 \le x \le 2$] consist of ca-bridged (4,4) layers with $[M_2(O_2CR)_4]$ as secondary building units that are pillared by the 1,4-dimb ligands into a unique 3D framework. The high-spin octahedral symmetry and the proportions of the mixed-metal ions were characterized by UV–vis spectroscopy. The compounds exhibit the onset of antiferromagnetic ordering at 7.5∼23 K, as well as weak ferromagnetism, spin-flop, and glassy behavior that result from the randomness of the mixed-metal pairs, magnetic anisotropy of the metallic cations, and antisymmetric exchange. The composites should be regarded as molecular alloys of the pure Ni(II) and Co(II) compounds. The magnetic behavior of the solid solutions shows unambiguously that the organic bridges, bond angles, and bond distances greatly influence the effective interactions and bring about cooperative magnetic behavior in the chiral 3D frameworks.

Introduction

One goal of crystal engineering is to develop novel materials with predefined and tunable properties, and molecule-based chiral magnets that manifest both magnetic ordering and optical activity represent a new frontier in the design of dual functional materials.[1] With such materials, chirality must be maintained at the molecular as well as the macroscopic levels. Another aspect of this field is the determination of key structural or electronic characteristics that govern the resulting magnetic ground states and their relation to modulated bulk magnetic properties. So far, only few examples of such magnets have been reported.[1b−i]

Among the class of metal carboxylates,[2] the tetracarboxylate-bridged dimetallic (e.g., Cu_2^{4+}, Zn_2^{4+}, and Mo_2^{4+}) paddlewheels have been envisaged as the secondary building units (SBUs) for the construction of metal-organic frameworks (MOFs) that display nanosized porosity and magnetic properties.[3,4] Although some dimeric $M_2(\mu\text{-}O_2CR)_4$-based

* Author to whom correspondence should be addressed. Fax: +86 20 8411-2245. E-mail: cxm@mail.sysu.edu.cn. (X.-M. Chen).
† Sun Yat-Sen University.
‡ Peking University.
§ GuangXi Normal University.

(1) (a) Rikken, G. L. A.; Raupach, E. *Nature* **2000**, *405*, 932. (b) Gao, E.-Q.; Yue, Y.-F.; Bai, S.-Q.; He, Z.; Yan, C.-H. *J. Am. Chem. Soc.* **2004**, *126*, 1419. (c) Inoue, K.; Kikuchi, K.; Ohba, M.; Okawa, H. *Angew. Chem., Int. Ed.* **2003**, *42*, 4810. (d) Imai, H.; Inoue, K.; Kikuchi, K.; Yoshida, Y.; Ito, M.; Sunahara, T.; Onaka, S. *Angew. Chem., Int. Ed.* **2004**, *43*, 5618. (e) Wen, H.-R.; Wang, C.-F.; Song, Y.; Zuo, J.-L.; You, X.-Z. *Inorg. Chem.* **2005**, *44*, 9039. (f) Feyerherm, R.; Loose, A. *Phys. Rev.* **2004**, *69*, 134427. (g) Liu, W.-L.; Song, Y.; Li, Y.-Z.; Zou, Y.; Dang, D.-B.; Ni, C.-L.; Meng, Q.-J. *Chem. Commun.* **2004**, 2348. (h) Coronado, E.; Galán-Mascarós, J. R.; Gómez-García, C. J.; Martínez-Ferrero, E.; Almeida, M.; Waerenborgh, J. C. *Eur. J. Inorg. Chem.* **2005**, 2064. (i) Telfer, S. G.; Sato, T.; Kuroda, R.; Lefebvre, J.; Leznoff, D. B. *Inorg. Chem.* **2004**, *43*, 421.
(2) Rao, C. N. R.; Natarajan, S.; Vaidhyanathan, R. *Angew. Chem., Int. Ed.* **2004**, *43*, 1466.
(3) (a) Doedens, R. J. *Prog. Inorg. Chem.* **1976**, *21*, 209 and references therein. (b) Carlin, R. L. *Magnetochemistry*; Springer-Verlag: Berlin, 1986. (c) Del Sesto, R. E.; Arif, A. M.; Miller, J. S. *Inorg. Chem.* **2000**, *39*, 4894.
(4) (a) Cotton, F. A.; Lin, C.; Murillo, C. A. *Acc. Chem. Res.* **2001**, *34*, 10 and 758. (b) Chui, S. S.-Y.; Lo, S. M.-F.; Charamant, J. P. H.; Orpen, A. G.; Williams, I. D. *Science* **1999**, *283*, 1148. (c) Maspoch, D.; Ruiz-Molina, D.; Wurst, K.; Domingo, N.; Cavallini, M.; Biscarini, F.; Tejada, J.; Rovira, C.; Veciana, J. *Nat. Mater.* **2003**, *2*, 190. (d) Vos, T. E.; Liao, Y.; Shum, W. W.; Her, J.-H.; Stephens, P. W.; Reiff, W. M.; Miller, J. S. *J. Am. Chem. Soc.* **2004**, *126*, 11630.

10.1021/ic060520g CCC: $33.50
Published on Web 08/10/2006

MOFs of Co^{II} and Ni^{II} have also been structurally established, only a few studies have been devoted to their magnetic properties, which exhibit simple antiferromagnetic (AF) coupling without ordering as those observed in discrete metal complexes.[5,6]

Stable chiral dicarboxylate dianions can be used to connect magnetic metal ions and the SBUs into MOFs of Co^{II} and Ni^{II} that confer structural chirality at both the molecular and macroscopic levels. The enhancement of the strong magnetic intercluster interaction in the 3D network combined with the intrinsic properties of the SBU, therefore, presents a new strategy in the design of high T_c chiral magnets. Furthermore, the incorporation of a second type of metal ion in a large proportion into the crystal lattice of a MOF containing a single type of metal ion is theoretically and practically feasible,[7] leading to a solid solution that can be used to adjust the number or uniformity of the SBU linkages between metal centers, leading to a greater control of the ordering temperature.[12−14] Expectedly, the manipulation of physical properties by changing metal compositions in the solid solution is different from the manipulation of conductivity of semiconductors modulated by trivial doping.[7d] More importantly, the solid solution exhibits additional properties such as indices of refraction and color that can be precisely and reliably fine-tuned.[7] Our approach is to combine such chiral dicarboxylates and mixed-metal ions into a crystalline MOF material that should exhibit rich chemistry and, at the same time, is a potential molecular alloy, hence, allowing a systematic magnetic study of 3D MOFs featuring dimeric SBUs with the dimetallic compositions prepared under hydrothermal reaction conditions.[2,7,8]

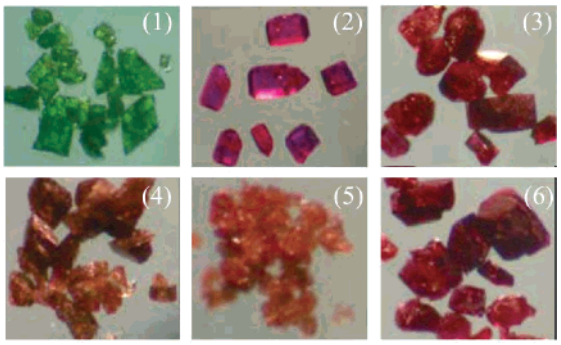

Figure 1. Photos of the crystals of **1**−**6**.

We describe herein the crystal structures and magnetic and spectral properties of six chiral, 3D MOFs $[M_2(ca)_2(1,4\text{-dimb})]_n$ [M = Ni^{II} (**1**), Co^{II} (**2**), $Co_{1/2}Ni_{1/2}$ (**3**), $Co^{II}_{1/4}Ni^{II}_{3/4}$ (**4**), $Co^{II}_{1/3}Ni^{II}_{2/3}$ (**5**), and $Co^{II}_{2/3}Ni^{II}_{1/3}$ (**6**); H_2ca = *D*-(+)-camphoric acid; 1,4-dimb = 1,4-di-(1-imidazolyl-methyl)-benzene] (Figure 1). These compounds possess dinuclear $M_2(\mu\text{-}O_2CR)_4$ SBUs with different Ni^{II}/Co^{II} ratios, a chiral dicarboxylate ca, and heterocyclic 1,4-dimb ligands, which were hydrothermically synthesized with the starting reagents in the stoichiometries of the corresponding products. Among them, **3**−**6** each contain both Ni^{II} and Co^{II} within the same crystal lattice and are referred to as a solid solution.[7,8]

Experimental Section

Materials and Measurements. All of the starting chemicals were of analytical reagent grade, except that 1,4-dimb was synthesized according to a literature procedure (see the Supporting Information), and used as received. Compounds **1**−**6** were synthesized directly through hydrothermal treatments using the starting reagents in the stoichiometries of the corresponding products at 170 °C for 7 days in high yields (ca. 90%).

Elemental analyses (C, H, and N) were performed on an Elementar Vario EL analyzer. IR spectra were recorded on a Nicolet Magna-IR 750 spectrometer equipped with a Nic-Plan microscope. Nuclear magnetic resonance spectra were obtained at room temperature with a Varian XL-300 spectrometer. To increase the signal-to-noise ratio, each spectrum was the average of at least 10 different scans. Solid UV−visible spectra were obtained in the 200∼800 nm range on a JASCO UVIDEC-660 spectrophotometer. Temperature- and field-dependent magnetic measurements were carried out on an Oxford MagLab 2000 magnetometer. Diamagnetic corrections were made with Pascal's constants. Thermogravimetric analysis (TGA) data were collected on a Perkin-Elmer TGS-2 analyzer in flowing air at a heating rate of 10 °C min^{-1} by heating microcrystals of **1**−**6**. X-ray powder diffraction data were collected on a Rigaku D/max-IIIA powder X-ray diffractometer. The relative molar ratios of Co/Ni in the mixed-metal crystals (**3**−**6**) were determined, using a Sciex ELAN inductively coupled plasma spectrometer on the crystals and the residual reaction solutions, to be 1.02:1, 1:2.93, 1:2.07, and 1.94:1, respectively, which have also been confirmed by X-ray photoelectron spectroscopy analysis on the surfaces of the crystals.

Crystallographic Studies. The single-crystal diffraction data were collected on a Bruker Smart Apex CCD diffractometer with graphite monochromated Mo Kα radiation (λ = 0.710 73 Å) at room temperature, and the absorption corrections were applied by

(5) (a) Moulton, B.; Abourahma, H.; Bradner, M. W.; Lu, J. J.; McManus, G. J.; Zaworotko, M. J. *Chem. Commun.* **2003**, 1342. (b) Lee, S. W.; Kim, H. J.; Lee, Y. K.; Park, K.; Son, J.-H.; Kwon, Y.-U. *Inorg. Chim. Acta* **2003**, *353*, 151. (c) Lee, D. W.; Hung, P.-L.; Spingler, B.; Lippard, S. J. *Inorg. Chem.* **2002**, *41*, 521.
(6) (a) Eremenko, I. L.; Nefedov, S. E.; Sidorov, S. E.; Golubnichaya, M. A.; Danilov, P. V.; Ikorskii, P. V.; Shvedenkov, Y. G.; Novotortsev, V. M.; Moiseev, I. I. *Inorg. Chem.* **1999**, *38*, 3764. (b) Lei, X.-L.; Shang, M.-Y.; Fehlner, T. P.; Werner, R.; Haase, W.; Hautot, D.; Long, G. J. *J. Organomet. Chem.* **1997**, *541*, 57.
(7) (a) Noveron, J. C.; Lah, M. S.; Sesto, R. E. D.; Arif, A. M.; Miller, J. S.; Stang, P. J. *J. Am. Chem. Soc.* **2002**, *124*, 6613. (b) MacDonald, J. C.; Dorrestein, P. C.; Pilley, M. M.; Foote, M. M.; Lundburg, J. L.; Henning, R. W.; Schultz, A. J.; Manson, J. L. *J. Am. Chem. Soc.* **2000**, *122*, 11692. (c) Pereira, C. L. M.; Pedroso, E. F.; Stumpf, H. O.; Novak, M. A.; Ricard, L.; Ruiz-García, R.; Rivière, E.; Journaux, Y. *Angew. Chem., Int. Ed.* **2004**, *43*, 955. (d) Archer, P. I.; Radovanovic, P. V.; Heald, S. M.; Gamelin, D. R. *J. Am. Chem. Soc.* **2005**, *127*, 14471.
(8) Itoh, K.; Kinoshita, M. *Molecular Magnetism, New Magnetic Materials*; Gordon Breach-Kodansha: Tokyo, 2000.
(9) (a) *SMART*, version 5.0; Bruker AXS: Madison, WI, 1998. *SAINTplus*, version 6.0; Bruker AXS: Madison, WI, 1999. *SHELXTL*, version 6.1; Bruker AXS: Madison, WI, 2001. (b) Blessing, R.; *Acta Crystallogr., Sect. A* **1995**, *51*, 33. (c) Spek, A. L. *PLATON, A Multipurpose Crystallographic Tool*; Utrecht University: Utrecht, The Netherlands, 1999.
(10) Batten, S. R.; Robson, R. *Angew. Chem., Int. Ed.* **1998**, *37*, 1460.
(11) (a) Figgis, B. N. In *Comprehensive Coordination Chemistry*; Wilkinson, G., Ed.; Pergamon: New York, 1987; Vol. 1, p 259. (b) Carlin, R. L. *Magnetochemistry*; Springer: Berlin, 1986.
(12) (a) Sun, H.-L.; Wang, Z.-M.; Gao, S. *Inorg. Chem.* **2005**, *44*, 2169. (b) Wang, X.-Y.; Wei, H.-Y.; Wang, Z.-M.; Chen, Z.-D.; Gao, S. *Inorg. Chem.* **2005**, *44*, 572.
(13) Zeng, M.-H.; Zhang, W.-X.; Sun, X.-Z.; Chen, X.-M. *Angew. Chem., Int. Ed.* **2005**, *44*, 3079.
(14) Kahn, O. *Molecular Magnetism*; VCH Publishers: New York, 1993; p 322.

Table 1. Summary of Crystallographic Data for **1**−**6**

compound	**1**	**2**	**3**
formula	$Ni_2C_{34}H_{42}N_4O_8$	$Co_2C_{34}H_{42}N_4O_8$	$CoNiC_{34}H_{42}N_4O_8$
fw	752.14	752.58	752.36
cryst syst	monoclinic	monoclinic	monoclinic
space group	$P2_1$	$P2_1$	$P2_1$
a (Å)	10.194(1)	10.226(1)	10.213(6)
b (Å)	12.679(2)	13.012(2)	12.886(8)
c (Å)	13.776(2)	13.551(2)	13.620(9)
β (deg)	90.954(2)	90.749(2)	90.845(1)
V (Å^3)	1780.1(4)	1802.8(4)	1792.3(2)
D_{calcd} (g/cm^3)	1.403	1.386	1.394
Z	2	2	2
R/wR_2 (obsd data)	0.0563/0.1548	0.0391/0.1399	0.0482/0.1297
flack parameter	0.19(4)	−0.05(3)	0.15(3)

compound	**4**	**5**	**6**
formula	$Co_{1/2}Ni_{3/2}C_{34}H_{42}N_4O_8$	$Co_{2/3}Ni_{4/3}C_{34}H_{42}N_4O_8$	$Co_{4/3}Ni_{2/3}C_{34}H_{42}N_4O_8$
fw	752.25	752.28	752.43
cryst syst	monoclinic	monoclinic	monoclinic
space group	$P2_1$	$P2_1$	$P2_1$
a (Å)	10.230(8)	10.213(1)	10.233 (7)
b (Å)	12.823(1)	12.829(1)	12.923(9)
c (Å)	13.628(1)	13.651(1)	13.608(9)
β (deg)	90.812(1)	91.049(2)	90.924(1)
V (Å^3)	1787.5(2)	1788.2(3)	1799.3(2)
D_{calcd} (g/cm^3)	1.401	1.401	1.389
Z	2	2	2
R/wR_2 (obsd data)	0.0676/0.1665	0.0805/0.2142	0.0517/0.1335
flack parameter	0.18(4)	0.37(6)	0.05(4)

SADABS.[9] The space group was determined from the systematic absences and further verified by the refinement results and PLATON.[9] The structures were solved by direct methods and refined using a full-matrix least-squares technique with SHELXL-97.[9] All non-hydrogen atoms were refined with anisotropic displacement parameters, whereas the hydrogen atoms of the ligands were placed at idealized positions and refined as riding atoms. Experimental details of the X-ray analyses are provided in Table 1. Selected bond distances and angles are listed in Table 2.

Results and Discussion

Crystal Structures. Compounds **1**−**6** are isomorphous, crystallizing in the chiral space group $P2_1$ with only slight differences in their unit-cell dimensions (by 0.33 Å, 2.6%) and volumes (by 22.6 Å^3, 1.3%) (Table 1). As shown in Figure 2, the dimeric SBU in **1** comprises two grossly distorted octahedral Ni^{II} atoms [Ni−N, 1.992(7) or 2.011(6) Å; Ni−O, 2.013(5)−2.295(6) Å] bridged by two bis-bidentate and two bis-tridentate carboxylate ends of the ca ligands, featuring an unusually short intradimer Ni1···Ni2 distance of 2.708(1) Å. Similar interatomic distances (Table 2) are noted for **2**−**6** with different proportions of Co^{II} and Ni^{II}. The SBUs are interlinked by the ca ligands into undulating (4,4) layers, which are further pillared by the 1,4-dimb ligands into a noninterpenetrating 3D motif (Figure 2) with the 1,4-dimb phenyl groups located in the free space between the layers (Chart 1) for compact packing. Owing to the steric hindrance of the chiral dicarboxylate, the entity charge balance, and coordination mode of the metal ion, the ca ligand should find it difficult to form a chiral 3D, SBU-based structure in the absence of 1,4-dimb. In fact, the appropriate degree of chemical flexibility of subsidiary ligand 1,4-dimb is probably favorable for a self-filling structure.[10]

Dimetal Solid Solution. The isostructural nature of **1** and **2**, which contain different bivalent transition metals (Ni^{II} and Co^{II}), suggests that one type of metal ion can be replaced by another without disruption of the lattice, so that the same 3D MOF would be retained when using different mixtures of Ni^{II} and Co^{II}. Through hydrothermal treatments, the other compounds **3**−**6** were obtained. As X-ray diffraction cannot readily distinguish between Ni^{II} and Co^{II}, they appear to be delocalized on the same site in the lattice and have a relative ratio corresponding to the reactants from which they were crystallized. Refinements on the occupancies at the metal centers indicated the ratios of Ni^{II} and Co^{II} to be 50:50%, 75:25%, 67:33%, and 33:67% for **3**−**6**, respectively. Meanwhile, there is no evidence that ordering of the metal ions in **3**−**6** has been found according to the magnetic measurements. These mixed-metal compositions show unambiguously that the bond angles and distances greatly influence the superexchange interactions.

Such kinds of materials, being referred to as solid solutions,[8] contain two different types of transition metals within the same single crystals. Our synthetic approach should be useful in the context of crystal engineering with regard to the design of materials.[8] Solid solutions are now considered a new class of materials exhibiting properties that can be altered systematically as a function of the types and relative ratios of transition metals, which can also be expected to have properties such as index of refraction and color.[8]

UV−Visible Spectra. Electronic spectra of phase-pure microcrystal samples of **1**−**6** and the two ligands are shown in Figure 3. Compound **1** shows three broad absorption bands in the 200∼800 nm range {one centered at 210 nm (ligands $n \rightarrow \pi^*$) with shoulders at 210∼225 nm, being contributed

Table 2. Selected Bond Lengths (Å) and Bond Angles (deg) for **1**−**6**

compounds[a]	1	2	3	4	5	6
			Bond Lengths			
M1−O	2.013(5)	2.010(3)	2.013(3)	2.005(6)	1.97(1)	2.015(4)
	2.019(5)	2.023(3)	2.021(4)	2.017(7)	2.03(1)	2.019(5)
	2.059(6)	2.041(4)	2.195(4)	2.077(8)	2.10(1)	2.084(5)
	2.110(6)	2.270(4)	2.088(4)	2.134(7)	2.18(1)	2.211(5)
	2.284(6)	2.409(4)	2.335(4)	2.340(8)	2.29(1)	2.348(6)
M2−O	2.018(5)	2.017(3)	2.015(4)	2.004(7)	2.00(1)	2.012(4)
	2.036(5)	2.029(3)	2.034(3)	2.019(6)	2.04(1)	2.032(4)
	2.046(6)	2.073(4)	2.036(5)	2.028(8)	2.05(1)	2.034(6)
	2.109(6)	2.284(4)	2.198(4)	2.166(8)	2.14(1)	2.216(5)
	2.295(6)	2.363(4)	2.360(4)	2.321(7)	2.38(1)	2.371(6)
M1−N	2.015(6)	2.040(4)	2.028(5)	2.037(8)	2.08(1)	2.027(6)
M2−N	1.992(6)	2.053(4)	2.025(5)	1.998(9)	1.988(1)	2.037(6)
M1−M2	2.708(1)	2.874(1)	2.795(1)	2.754(2)	2.774(2)	2.816(1)
			Bond Angles			
O1−M1−O6	168.2(2)	161.2(1)	164.0(1)	166.6(2)	163.7(2)	165.7(4)
O1−M1−N1	94.6(2)	95.6(2)	95.1(2)	94.7(3)	94.9(2)	96.3(5)
O1−M1−O7d	91.3(2)	96.1(1)	94.2(2)	92.7(3)	94.4(2)	93.6(4)
O1−M1−O8d	84.7(2)	85.5(1)	85.2(2)	85.5(3)	84.9(2)	86.3(4)
O1−M1−O4e	87.0(2)	83.4(2)	85.3(2)	86.5(3)	85.0(2)	87.9(4)
O6−M1−N1	95.1(2)	96.1(2)	96.4(2)	95.9(3)	96.6(2)	94.8(5)
O6−M1−O7d	92.8(2)	94.3(1)	93.5(2)	92.6(3)	93.6(2)	91.9(4)
O6−M1−O8d	87.8(2)	86.6(2)	86.7(2)	86.7(3)	87.0(2)	85.0(4)
O4e−M1−O6	86.2(2)	82.1(1)	83.4(2)	85.0(3)	83.4(2)	83.4(4)
O7d−M1−N1	103.8(2)	166.3(2)	105.6(2)	104.0(3)	105.6(2)	105.9(5)
O8d−M1−N1	163.9(2)	107.4(2)	164.6(2)	163.5(3)	164.8(2)	166.1(5)
O4e−M1−N1	91.0(2)	89.6(2)	90.7(2)	92.1(3)	90.6(2)	89.1(5)
O7d−M1−O8d	60.2(2)	59.0(1)	59.1(1)	59.5(3)	59.3(2)	60.3(3)
O4e−M1−O7d	165.2(2)	162.9(1)	163.6(1)	163.9(2)	163.7(2)	164.6(4)
O4e−M1−O8d	105.0(2)	104.0(1)	104.6(2)	104.4(2)	104.5(2)	104.6(3)
O2−M2−O5	165.3(2)	161.0(1)	163.5(1)	164.8(2)	162.6(2)	163.6(3)
O2−M2−N4a	95.4(3)	94.5(2)	94.5(2)	94.4(3)	93.9(2)	95.2(5)
O2−M2−O8d	84.5(2)	83.5(1)	85.0(2)	85.6(3)	83.9(2)	86.3(5)
O2−M2−O3e	93.1(2)	95.3(2)	94.2(2)	93.1(3)	94.8(2)	94.7(4)
O2−M2−O4e	84.5(2)	84.1(1)	84.4(1)	84.7(3)	84.3(2)	85.9(4)
O5−M2−N4a	96.7(3)	98.0(2)	97.6(2)	97.4(3)	98.3(2)	97.2(5)
O5−M2−O8d	86.8(2)	81.9(2)	83.4(2)	84.5(3)	83.5(2)	82.3(4)
O3e−M2−O5	92.1(2)	94.7(2)	93.3(2)	93.2(3)	93.5(2)	92.4(4)
O4e−M2−O5	86.3(2)	87.3(2)	86.9(1)	86.4(3)	87.1(2)	85.2(4)
O8d−M2−N4a	92.4(3)	91.4(2)	91.6(2)	91.7(3)	91.4(2)	93.7(4)
O3e−M2−N4a	103.5(3)	107.0(2)	105.8(2)	104.3(3)	106.6(2)	104.6(4)
O4e−M2−N4a	162.7(3)	165.2(2)	164.5(2)	164.1(3)	164.6(2)	163.5(4)
O3e−M2−O8d	164.1(2)	161.6(1)	162.6(2)	164.0(3)	162.1(2)	161.5(4)
O4e−M2−O8d	104.8(2)	103.0(1)	103.7(1)	104.0(3)	103.6(2)	102.7(3)
O3e−M2−O4e	59.4(2)	58.7(1)	59.0(1)	60.0(2)	58.5(2)	59.0(3)

[a] Symmetry codes: a = $-1+x, -1+y, z$; b = $1+x, 1+y, z$; c = $-x, -1/2+y, 1-z$; d = $-x, -1/2+y, 2-z$; e = $-x, 1/2+y, 1-z$.

by the ligands, the second centered at 410 nm [$^3T_{1g}(p) \leftarrow {}^3A_{2g}$], and the third centered at 690 nm [$^3T_{1g}(F) \leftarrow {}^3A_{2g}$], which are typical for octahedrally coordinated Ni^{II} complexes.[11] Compound **2** also shows three broad absorption bands {one centered at 210 nm (ligands n $\rightarrow \pi^*$) with shoulders, the second at 470 nm [$^4T_{1g}(F) \rightarrow {}^4T_{2g}(F)$] with a shoulder at 530 nm [$^4T_{1g}(F) \rightarrow {}^4T_{1g}(P)$], and the third at 740 nm [$^4T_{1g}(F) \rightarrow {}^4A_{2g}(F)$], the bands again being typical of high-spin, octahedrally coordinated Co^{II} complexes.[11] The spectral features of the solid solutions **3**−**6** are, not surprisingly, similar to each other and are practically superpositions of **1** and **2** with slight differences in the intensities arising from the relative Co^{II}/Ni^{II} ratios, in which those of the Co-rich crystals are more like those of **2**, whereas those of the Ni-rich crystals are more like those of **1**.

Thermal Stability of 1−6. The thermogravimetric analyses of **1**−**6** (see Figure S1, Supporting Information) showed similar decomposition behaviors. Both **1** and **2** remained stable up to ca. 290 °C, indicating high thermal stability of the frameworks. However, the equal composite **3** shows less stability (at ca. 250 °C), whereas **4**−**6** were more stable with a temperature of ca. 330 °C. Pyrolysis of the organic ligands in **1**−**6** occurred in the temperature ranges of 290−403, 290−410, 250−429, 330−424, and 330−425 °C, respectively. The final residuals are Ni_2O_3 for **1**, Co_2O_3 for **2**, and M_2O_3 for **3**−**6** (M = Co, Ni) (weight left found: 21.9, 21.9, 22.0, 21.5, 21.7, and 21.8% for **1**−**6**, respectively, compared to the calculated weight of 22.0% for all). The thermal stabilities of **1**−**6** are better than those of other molecule-based chiral magnets containing azide or cyanide ions.[1a−d]

Magnetic Studies. The magnetic data were measured on the phase-pure crystals. The dc magnetization data of **1**−**6** are shown in Figure 4. The χ_M increases to a rounded maximum at ca. 24 K for **1**, 7.5 K for **2**, and ca. 16 K for **3**, whereas the μ_{eff} value decreases monotonically upon cooling (Figure S2, Supporting Information). For **4**−**6**, χ_M keeps increasing with cooling without a maximum value; the values of μ_{eff} remain almost constant upon cooling from room temperature to 50 K and, then, decrease on further cooling.

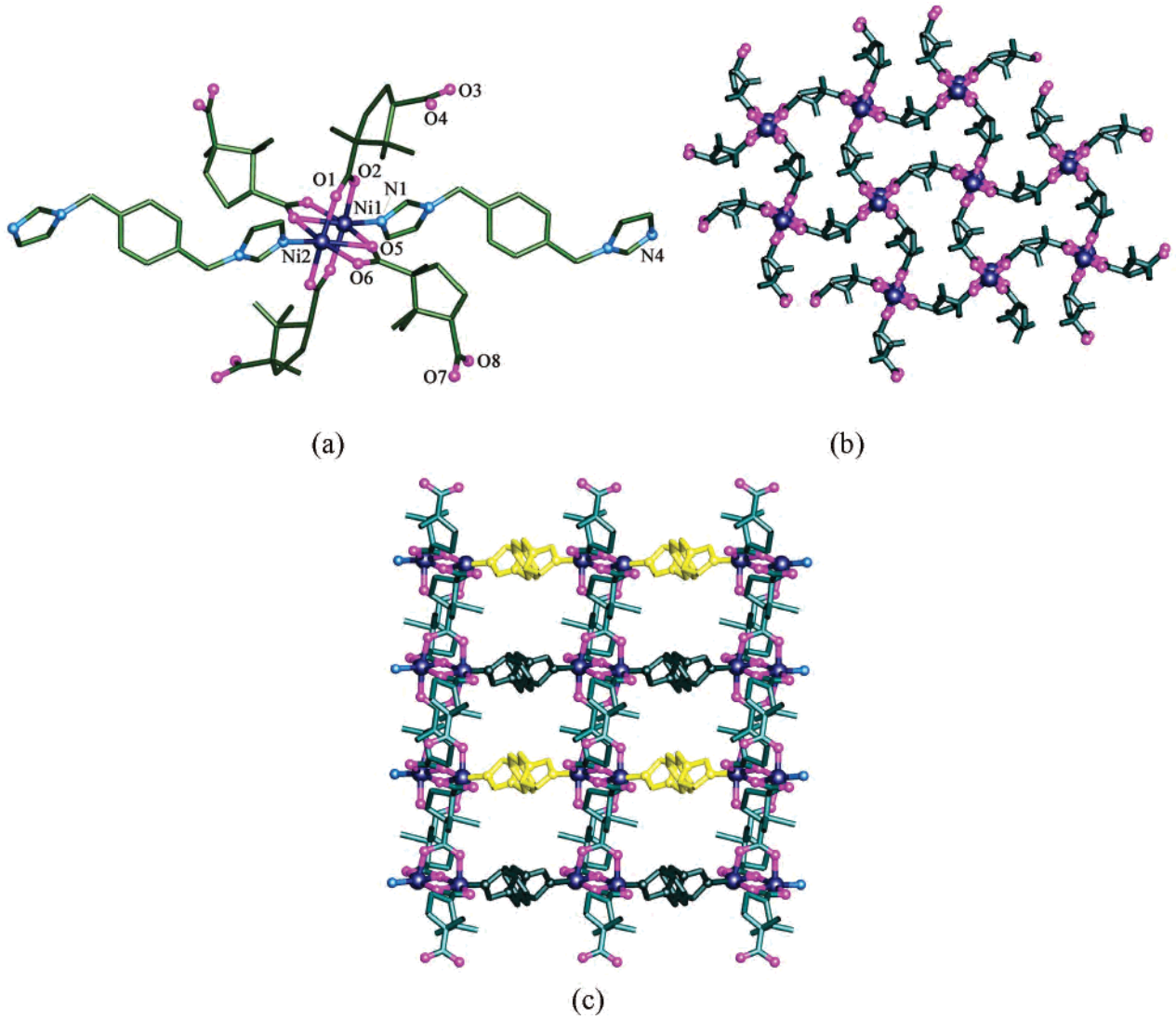

Figure 2. Perspective views of the SBU (a), (4,4) layer (b), and 3D MOF (c) in **1**. Color codes for C, N, O, and Ni atoms are greenish black, blue, pink, and indigo-blue; the yellow and dark cyan show the two different packing directions of 1,4-dimb.

Chart 1. Schematic Representation of the 1,4-dimb Ligands Bridging Adjacent Layers in Two Different Directions into a 3D MOF

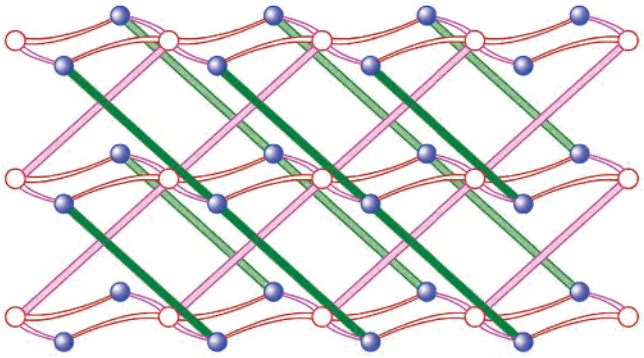

The temperature dependence of χ_M for **1** and **2** can be attributed to the intra- and interdimer interactions J and J', respectively.[12−14] Because the distances between two adjacent SBUs are considerably longer than the intradimer M1···M2 separation, the interdimer exchange interactions (J') must be very weak. As an exact mathematical expression to evaluate the susceptibility of such a complex 3D system of **1** has not been developed, we have used an admittedly simple dimer

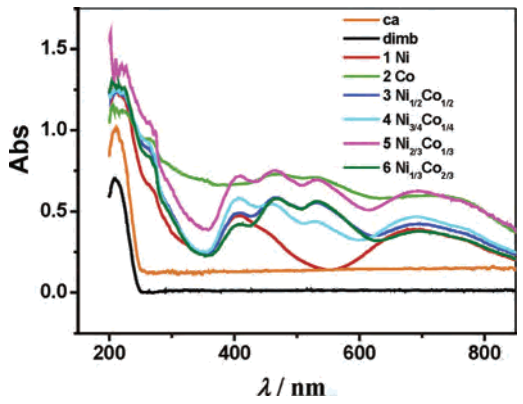

Figure 3. Solid UV−visible spectra of **1**−**6** and the ligands.

model instead ($\hat{H}_{ex} = -J\hat{S}_1\hat{S}_2$).[14] A least-squares fit of the data above 54 K gave $J = -21.98$ cm^{-1}, $Z'J' = -0.27$ cm^{-1}, and $g = 2.61$ for **1** (Figure S3, Supporting Information), indicating a relatively strong antiferromagnetic intradimer Ni^{II} interaction, which is similar to those observed in several related octahedrally coordinated Ni^{II} complexes with similar binuclear cores.[15,16] It must be noted that the

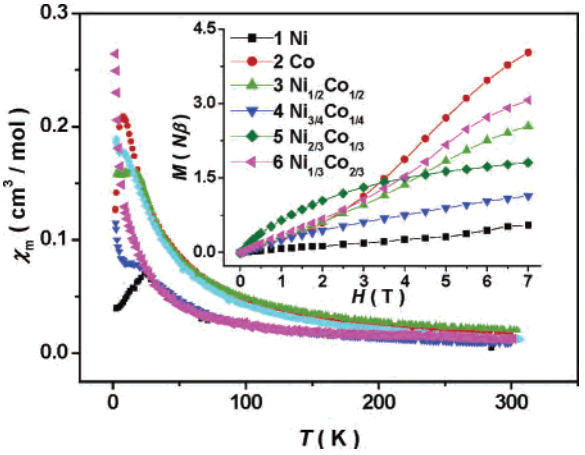

Figure 4. χ_M-T plots for **1** per Ni^{II}_2 at 30 kOe (black), **2** per Co^{II}_2 at 10 kOe (red), **3** per CoNi at 10 kOe (green), **4** per $Co_{1/2}Ni_{3/2}$ at 30 kOe (blue), **5** per $Co_{2/3}Ni_{4/3}$ at 20 kOe (magenta), and **6** per $Co_{4/3}Ni_{2/3}$ at 20 kOe (cyan). Inset: field dependence of magnetization for **1**−**6** at 1.8 K at 0∼70 kOe.

exchange interaction within Co^{II} complexes is difficult to accurately estimate because of the effects of spin−orbit coupling. Taking into account spin-only coupling for the dimer ($\hat{H}_{ex} = -J\hat{S}_1\hat{S}_2$), a good fit to the data above 50 K was achieved for **2** ($J = -5.76$ cm^{-1}, $Z'J' = -0.01$ cm^{-1}, and $g = 2.4$; Figure S4, Supporting Information).[15,16] The J values of **1** and **2** show $|J_{NiNi}| > |J_{CoCo}|$, which is in accord with the positions of the maxima in χ_M versus T curves. From a comparison of J_{NiNi} with J_{CoCo}, the relative predominance of the antiferromagnetic contribution tends to be weakened with an increase in the number of unpaired electrons in the metal(II) t_{2g} orbital.[16]

The $\chi_{ac}(T)$ data of **1**−**6** all show a very broad peak of the χ' components of the magnetization. All of the Ni-rich compounds have more absorptive peaks than those of the Co-rich compounds, in accord with the dc measurements (Figure 5). These data allow a precise determination of the temperature at which spontaneous magnetization occurs with the broad peak of χ' under 277 Hz, namely, T^* at 19.5, 8, 15, 14, 13, and 10 K for **1**−**6**, respectively. There is weak frequency dependence in the $\chi_{ac}(T)$ response along with a glasslike behavior of all Ni-containing compounds around the ordering temperature. The shift of the peak temperature (T_P) of the χ' peak positions as measured by a parameter $\phi = \Delta T_p/[T_p\Delta(\log f)]$ is 0.005, 0.022, 0.026, 0.021, and 0.025 for **1**, **3**−**6**, respectively.[17,18] The glassy behavior may result from metal ion disorder or defects in the crystal structure.[18]

Significant divergences between the zero-field-cooled (ZFC) and field-cooled (FC) magnetizations in an applied field of 200 Oe (Figure 6 and Table 3) observed below 23, 14, 12.5, 11.0, and 11.5 K for **1**, **3**−**6**, respectively, might be attributed to canted antiferromagnetic behavior. Hysteresis loops were also observed at 1.8 K showing a coercive field H_{cr} of 913, 205, 67, 348, and 97 Oe, and a M_r of 1758, 40, 18, 284, and 26 Oe for **1**, **3**−**6**, respectively (Figure S5, Supporting Information). These are in agreement with the above results and confirm the occurrence of a weak ferromagnetic behavior.

Table 3. Summary of the Magnetic Properties for **1**−**6**

	1	**2**	**3**	**4**	**5**	**6**
H_c/Oe	913		205	67	348	97
M_r/Oe	1758		40	18	284	26
M ($N\beta$/mol at 70 kOe)	0.55	4.03	2.54	1.14	1.81	3.07
T_{div} (at 200 Oe FC−ZFC)	23.0	7.5	14	12.5	11.0	11.5
T^* (K, ac 277 Hz)	19.5	8.0	15.0	14.0	13.2	10.0

For the Ni-rich compounds (**1**, **4**, and **5**), the magnetization at 1.8 K increased almost linearly and slowly with the applied field up to 70 kOe. However, it reached 0.55, 1.14, and 1.81 $N\beta$/mol at 70 kOe but did not become saturated (inset of Figure 4). For the Co-rich compounds, the field-dependent magnetization showed a pronounced sigmodial shape and reached 4.03, 2.54, and 3.07 $N\beta$/mol at 70 kOe for **2**, **3**, and **6**, respectively, but did not saturate as well, which implies a spin-flop transition. The $\chi_{dc}(T)$ measurements for **2** at several dc fields (Figure 7) show that the higher the applied field, the larger the values of χ_{dc} below the order temperature, an observation that further confirms a specific field-dependence behavior, known as a spin-flop transition of **2**.[16] From different dc FC measurements, **3** also exhibits a weak spontaneous magnetization at lower fields (1 kOe) and shows a spin-flop transition to a spin-polarized state at high fields (>40 kOe). The above data demonstrate that the magnetic properties of **3** are rather complex, consisting of the features of both **1** and **2**, weak ferromagnetism and field-induced spin-flop transition. The properties are, however, not a simple addition of those of **1** and **2**.[16]

Cooperative Magnetic Behaviors. The phenomena are explained in terms of weak ferromagnetism caused by small, uncompensated AF spin-canting for **1** and antiferromagnetism with spin-flop for **2**.[1c,19] Such canting is commonly attributed to both a strong single-ion anisotropy of Ni^{II} and the Dzyaloshinsky−Moriya interaction that is symmetry-allowed because of the chiral structures.[20] In **2**, **3**, and **6**, the spin-flop behavior is influenced by the weak single-ion magnetic anisotropy of Co^{II}, which is consistent with the highly distorted octahedral environment of the high-spin Co^{II} (d^7).[11,16] Solid solutions **3**−**6** display both weak ferromagnetic and spin-flop behaviors, which may be ascribed to a summation of the behaviors of **1** and **2**. The Co-rich and

(15) (a) Hossain, M. J.; Yamasaki, M.; Mikuriya, M.; Kuribayashi, A.; Sakiyama, H. *Inorg. Chem.* **2002**, *41*, 4058. (b) Ginsberg, A. P.; Martin, R. L.; Brookes, R. W.; Sherwood, R. C. *Inorg. Chem.* **1972**, *11*, 2884.
(16) Sun, B.-W.; Song, G.; Ma, B.-Q.; Niu, D.-Z.; Wang, Z.-M. *J. Chem. Soc., Dalton Trans.* **2000**, 4187.
(17) (a) Manson, J. L.; Huang, Q.-Z.; Lynn, J. W.; Koo, H.-J.; Whangbo, M.-H.; Bateman, R.; Otsuka, T.; Wada, N.; Argyriou, D. N.; Miller, J. S. *J. Am. Chem. Soc.* **2001**, *123*, 162. (b) Carlin, R. L.; van Duyneveldt, A. J. *Acc. Chem. Res.* **1980**, *13*, 231. (c) Wang, X.-Y.; Wang, L.; Wang, Z.-M.; Su, G.; Gao, S. *Chem. Mater.* **2005**, *17*, 6369.
(18) Mydosh, J. A. *Spin Glasses: An Experimental Introduction*; Taylor and Francis: Washington, DC, 1993.
(19) (a) Lines, M. E. J. *Chem. Phys.* **1971**, *55*, 2977. (b) Spasojevic, V.; Kusigerski, V.; Sovilj, S. P.; Mrozinski, J. *J. Magn. Magn. Mater.* **2000**, *219*, 269.
(20) (a) Dzyaloshinsky, I. *Phys. Chem. Solids* **1958**, *4*, 241. (b) Moriya, T. *Phys. Rev.* **1960**, *120*, 91. (21) Lappas, A.; Wills, A. S.; Green, M. A.; Prassides, K.; Kurmoo, M. *Phys. Rev. B: Condens. Matter Mater. Phys.* **2003**, *67*, 144406.

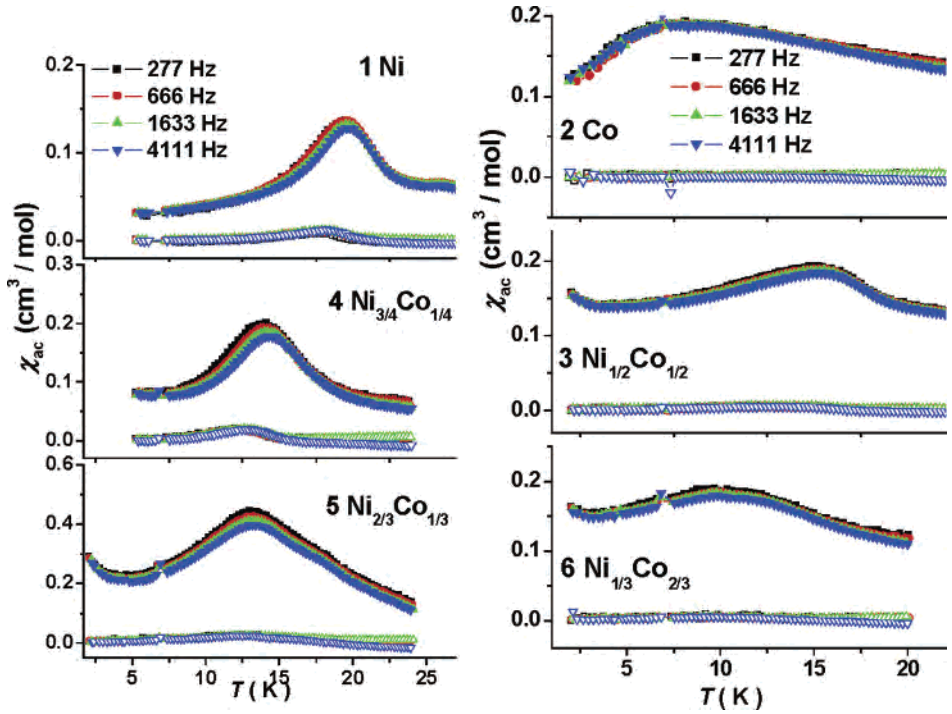

Figure 5. Temperature dependence of *ac* magnetic susceptibility (upper, χ'; lower, χ'') at different frequencies.

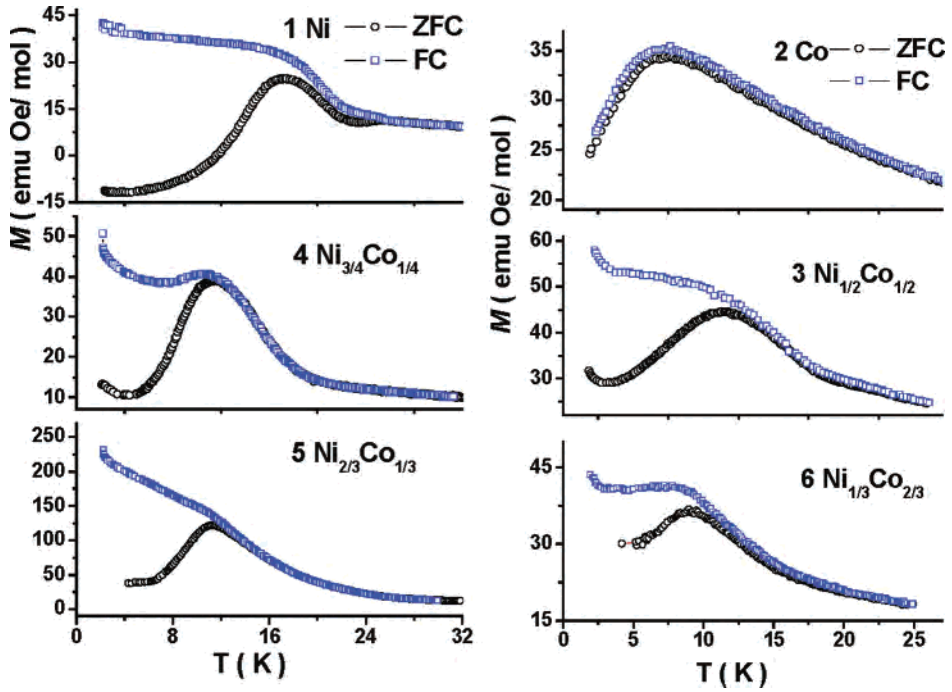

Figure 6. ZFC and FC magnetization at 200 Oe for **1**−**6**.

Ni-rich compounds show more pronounced effects of **2** and **1**, respectively. As a result of metal-ion modulation, the materials exhibit obvious changes in the magnetic ordering temperature [from 8 to 19.5 K (T*, at 277 Hz of χ'_{ac})] and large coercive fields [from 67 to 913 Oe and remnant magnetization ranging from 18 to 1758 Oe at 1.8 K]. Our results demonstrate that **1**−**6** comprise a class of compounds whose magnetic properties can be altered systematically as an approximately linear function of the types and relative ratios of metals (Figure 8).

The bulk magnetic behaviors of **1**−**6** are consistent with the cooperative interactions of the dimers in the 3D MOFs. The interactions are also probably modulated by the flexible organic bridges that enhance the magnetic intercluster interactions in the 3D MOF and that bring into existence the observed cooperative magnetic behaviors because the through-space separation of the dimers is not much different from that of the discrete dimeric molecular systems.[6] On the other hand, the magnetic behaviors of doped **3**−**6** show unambiguously that the organic bridges, bond angles, and

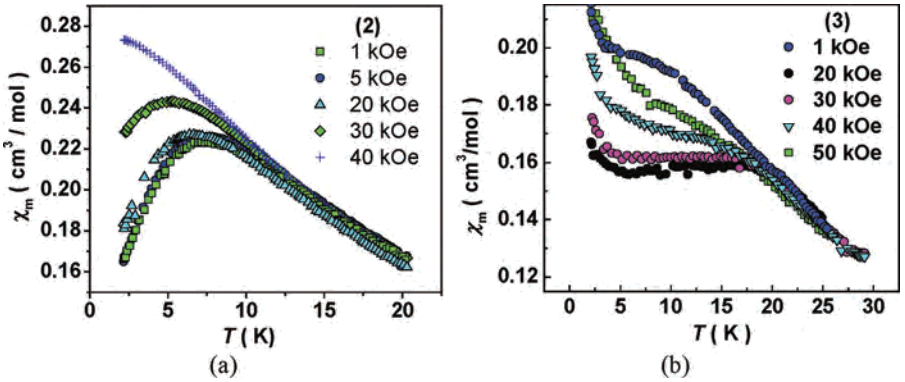

Figure 7. Field-cooled susceptibilities of **2** (a) and **3** (b) at different applied fields.

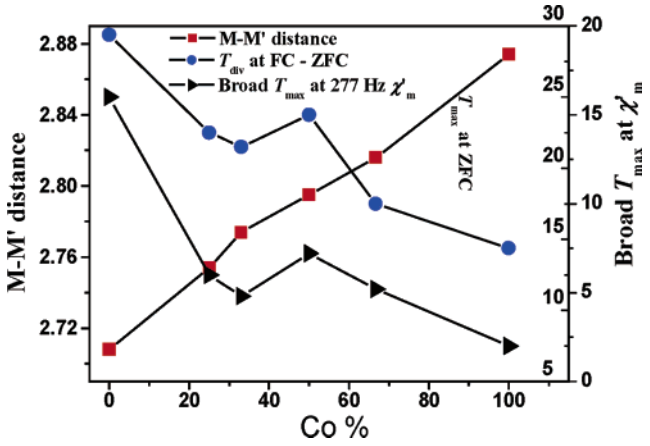

Figure 8. Correlations of the broad peak of χ' under 277 Hz, intradimer distance, and M/M′ molar ratio in **1**−**6**.

bond distances are not the only factors controlling the resulting magnetic ground states and that the different electronic configurations made by mixed-metal ions can tune the relative number and strength of AF interactions and magnetic anisotropy.[21] Although X-ray diffraction cannot readily distinguish between Ni^{II} and Co^{II}, analytical data confirm that the metal ions have a relative ratio directly corresponding to the starting reactants. However, there is still no reliable experimental evidence to support the ordering of the different dimers in **3**−**6**. As such, **3**−**6** should be regarded as magnetic molecular alloys of **1** and **2**, and our observation should be useful to an understanding of the balance between structural and electronic effects that influence and adjust magnetic ground states and bulk magnetic behavior.

(21) (a) Miyasaka, H.; Nakata, K.; Sugiura, K.; Yamashita, M.; Clérac, R. *Angew. Chem., Int. Ed.* **2004**, *43*, 707. (b) Miyasaka, H.; Nakata, K.; Lecren, L.; Coulon, C.; Nakazawa, Y.; Fujisaki, T.; Sugiura, K.; Yamashita, M.; Clérac, R. *J. Am. Chem. Soc.* **2006**, *128*, 3770.

Conclusions

We present in this work a new synthetic strategy for building structurally chiral molecular magnets by using flexible chiral carboxylates that feature unusually short intradimer metal−metal distances in the $M_2(\mu\text{-}O_2CR)_4$ SBUs. We have also demonstrated that MOFs of appropriate magnetic multinuclear SBUs are potential molecular magnetic alloy materials generated through crystal engineering using different metal compositions.[22] Such a strategy is envisaged to furnish simple or complex architectures that may have intrinsic properties and may lead to the generation of more interesting, adjustable magnetic and optical properties as well as to a better understanding of the cooperative effect between structural and electronic effects.[1,21,22]

Acknowledgment. This work was supported by NSFC (No. 20531070, 20561001, 20221101, and 20490210) and the Scientific and Technological Department of Guangdong Province (No. 04205405).

Supporting Information Available: Synthesis of 1,4-dimb; additional magnetic, TGA, and PXRD plots; and X-ray crystallographic files in CIF format for the structure determinations of **1**−**6**. This material is available free of charge via the Internet at http://pubs.acs.org.

IC060520G